

ARTICLE

Received 13 Oct 2014 | Accepted 22 May 2015 | Published 1 Jul 2015

DOI: 10.1038/ncomms8590

OPEN

Mechanically selflocked chiral gemini-catenanes

Sheng-Hua Li¹, Heng-Yi Zhang¹, Xiufang Xu¹ & Yu Liu¹

Mechanically interlocked and entangled molecular architectures represent one of the elaborate topological superstructures engineered at a molecular resolution. Here we report a methodology for fabricating mechanically selflocked molecules (MSMs) through highly efficient one-step amidation of a pseudorotaxane derived from dual functionalized pillar[5]arene (P[5]A) threaded by α,ω -diaminoalkane (**DA-*n***; $n = 3-12$). The monomeric and dimeric pseudo[1]catenanes thus obtained, which are inherently chiral due to the topology of P[5]A used, were isolated and fully characterized by NMR and circular dichroism spectroscopy, X-ray crystallography and DFT calculations. Of particular interest, the dimeric pseudo[1]catenane, named 'gemini-catenane', contained stereoisomeric *meso-erythro* and *dl-threo* isomers, in which two P[5]A moieties are threaded by two **DA-*n*** chains in topologically different patterns. This access to chiral pseudo[1]catenanes and gemini-catenanes will greatly promote the practical use of such sophisticated chiral architectures in supramolecular and materials science and technology.

¹Department of Chemistry, State Key Laboratory of Elemento-Organic Chemistry, Collaborative Innovation Center of Chemical Science and Engineering (Tianjin), Nankai University, Tianjin 300071, China. Correspondence and requests for materials should be addressed to Y.L. (email: yuliu@nankai.edu.cn).

Since the pioneering work by Frisch and Wasserman on chemical topology¹, mechanically interlocked and entangled molecular architectures have attracted much interest because of their fascinating topological features^{2,3} as well as the increasing influences on materials science and nanotechnology^{4–7}. Inspired partly by the mathematical, iconological and religious symbols, much progress has been made in the rational synthesis of the mechanically interlocked molecules (MIMs) with ever-growing complexity^{8–14}. A vast variety of bi- and multi-component MIMs, including $[n]$ rotaxanes ($n \geq 2$), $[n]$ catenanes ($n \geq 2$) and $[cn]$ daisy chains ($n \geq 2$)^{15–18}, have hitherto been synthesized. In contrast, the covalently linked single-component locked molecules, which may be called mechanically selflocked molecules (MSMs)¹⁹, have sporadically been reported. Typical examples of MSMs include pseudo[1]rotaxane^{20–22}, pseudo[1]catenane^{23,24}, pretzelane^{25,26}, double-lasso rotamacrocyclic^{27,28} and molecular figure-of-eight²⁹. Compared with the well-established MIMs, however, the construction of higher-order MSM systems still remains a challenge, mainly due to the lack of a convenient general synthetic route and the tremendous obstacles in both synthesis and characterization.

1-Hydroxybenzotriazole (HOBT), a widely used additive for peptide synthesis³⁰, has also been applied to the synthesis of cyclic peptides^{31,32}, which stimulated us to employ this reagent in the synthesis of pseudo[1]catenanes and single-component MSMs through amidation.

In this study, we have applied HOBT to the synthesis of a series of MSMs and found that the amidation mediated by HOBT serves as the essential step for constructing these sophisticated topologies. Intriguingly, when a long α,ω -diaminoalkane was reacted with pillar[5]arene-dicarboxylic acid in the presence of a condensation reagent (EDCI) and HOBT, a new member of the MSM family was obtained and eventually identified as a dually threaded pseudo[1]catenane, or ‘gemini-catenane’ in addition to a singly threaded pseudo[1]catenane, both of which are conformationally stable and inherently chiral.

Results

Synthetic approach to MSMs. The Pillar[5]arene (P[5]A) is a [1₅]paracyclophane derivative consisting of five 1,4-dialkoxycyclohexane units mutually connected at the 2- and 5-positions with a methylene bridge³³. The circular oxygen alleys at the both portals of pillararene, analogous to crown ether, strongly bind dicationic organic and difunctional guests^{34–37}. A1/A2-difunctionalized dimethylpillar[5]arene (DMP[5]A)³⁸ can be prepared by the partial oxidation of DMP[5]A^{39,40} and subsequent modification. Exploiting these features of P[5]A, we designed A1/A2-dicarboxylato-DMP[5]A (**4**) as the wheel of pseudorotaxane and α,ω -diaminoalkane as the axle. As shown in Fig. 1b, **4** was prepared from 1,4-dimethoxypillar[4]arene[1]hydroquinone (**3**) in 81% yield through alkylation with ethyl bromoacetate and the subsequent hydrolysis. Dicarboxylic acid **4** was reacted with 1,8-diaminooctane (**DA-8**) in the presence of 1-(3-dimethylaminopropyl)-3-ethylcarbodiimide hydrochloride (EDCI·HCl) (2.5 equiv.) and HOBT (2.5 equiv.) for 48 h in CHCl₃ at room temperature to afford **1a** as a white solid (melting point: 290–292 °C) in 51% isolated yield. The chemical structure of **1a** was fully characterized by ¹H NMR, ¹³C NMR, IR and HRMS spectroscopies and also by X-ray crystallography. In the IR spectra, the C=O stretching vibration was shifted from 1,730 cm⁻¹ in **4** to 1,681 cm⁻¹ in **1a**, indicating formation of the amide linkage (see Supplementary Figs 53 and 54). In the ¹H NMR spectra of **1a**, the signals of axle methylene protons were

greatly upfield-shifted to $\delta < 0$, as a consequence of the shielding effect of the pillararene’s aromatic rings (see Supplementary Fig. 5). The crystal structure of **1a** (Fig. 2a) unambiguously revealed the formation of pseudo[1]catenane, in which the pillararene ring is threaded by the octamethylene chain. Since this pseudo[1]catenane is planar-chiral as is the case with pillar[5]arene, the enantiomer pair was resolved by chiral HPLC. The first and second fractions collected showed mirror-imaged circular dichroism (CD) spectra (Supplementary Figs 68 and 69) and were assigned to (*pS*)- and (*pR*)- enantiomers of pseudo[1]catenane **1a**, respectively, by comparison with the theoretical CD spectra of P[5]A simulated by using the density functional theory (DFT)⁴¹.

Interestingly, two additional products eluted by more polar solvents upon chromatographic separation were isolated in 9 and 19% yield, respectively. The HRMS analyses revealed their parent peaks in the ‘dimer’ region at *m/z* 1,894.9295 and 1,894.9445, respectively (see Supplementary Figs 46 and 47). Possessing exactly the twofold mass of **1a**, these ‘dimeric’ products were assignable either to non-threaded 2:2 monocyclic dimers of **4** with **DA-8** or to selflocked gemini-catenanes **2a** and **2’a**. The possibility of the non-threaded cyclodimers was immediately excluded on the basis of the unusually upfield-shifted octamethylene protons (Supplementary Fig. 29). As a natural consequence of the planar chirality of pillararene³⁸ (Fig. 1b) and pre-assembled pseudorotaxane **4** used as a substrate in the present synthesis, the gemini-catenane generated therefrom should contain one S₂-symmetric ‘erythro’ and two C₂-symmetric ‘threo’ isomers. The catenane structure is obvious from the unusual upfield shifts of the octamethylene protons a–d in the ¹H NMR spectra (Supplementary Fig. 29). More crucially, the two sets of protons a–d, which are equivalent to each other in **1a**, are desymmetrized to give two significantly split series of protons a–d and a’–d’ in gemini-catenanes **2a** and **2’a**, revealing inequivalent magnetic environment for each series of the protons. Thus, the protons b–d are more deeply embedded into the pillararene cavity and suffer stronger shielding effects than the protons b’–d’ to show upfield shifts up to –1.97 p.p.m. in **2a** and even to –2.33 p.p.m. in **2’a**.

The ¹³C NMR spectra of **2a** and **2’a** confirm the above assignment. As can be seen from Fig. 3, the carbonyl carbon (C_x) and the two methylene carbons (C_a and C_y) adjacent to the amide group in **1a** give single peaks, reflecting the equivalent magnetic environment for each of these carbons. In sharp contrast, all of the C_a, C_x and C_y signals significantly split in both **2a** and **2’a**, indicating that the two amide groups are no longer equivalent in these molecules due to the gemini-catenane structure.

Chirality of gemini-catenanes. The HRMS, ¹H NMR and ¹³C NMR spectral analyses have unambiguously proven the gemini-catenane structure of **2a** and **2’a**, but did not allow us to discern these two stereoisomeric molecules. Nevertheless, their chiral structures and the relevant chiroptical properties enabled us not only to discern them but also to unequivocally assign their absolute configurations with the aid of circular dichroism (CD) spectra. From the symmetry point of view, gemini-catenane is either S₂-symmetric (achiral) ‘erythro’ or C₂-symmetric (chiral) ‘threo’, the former of which has a centre of symmetry and exists as a single meso-isomer, while the latter has no centre or plane of symmetry and therefore exists as a pair of enantiomers^{42–44}. Knowing that, we performed the chiral HPLC analysis of these gemini-catenanes to find a single peak at 8.6 min for **2a** but two well-separated peaks at 6.2 and 9.2 min for **2’a** under the identical conditions (see Fig. 4a,b), revealing that the former is achiral

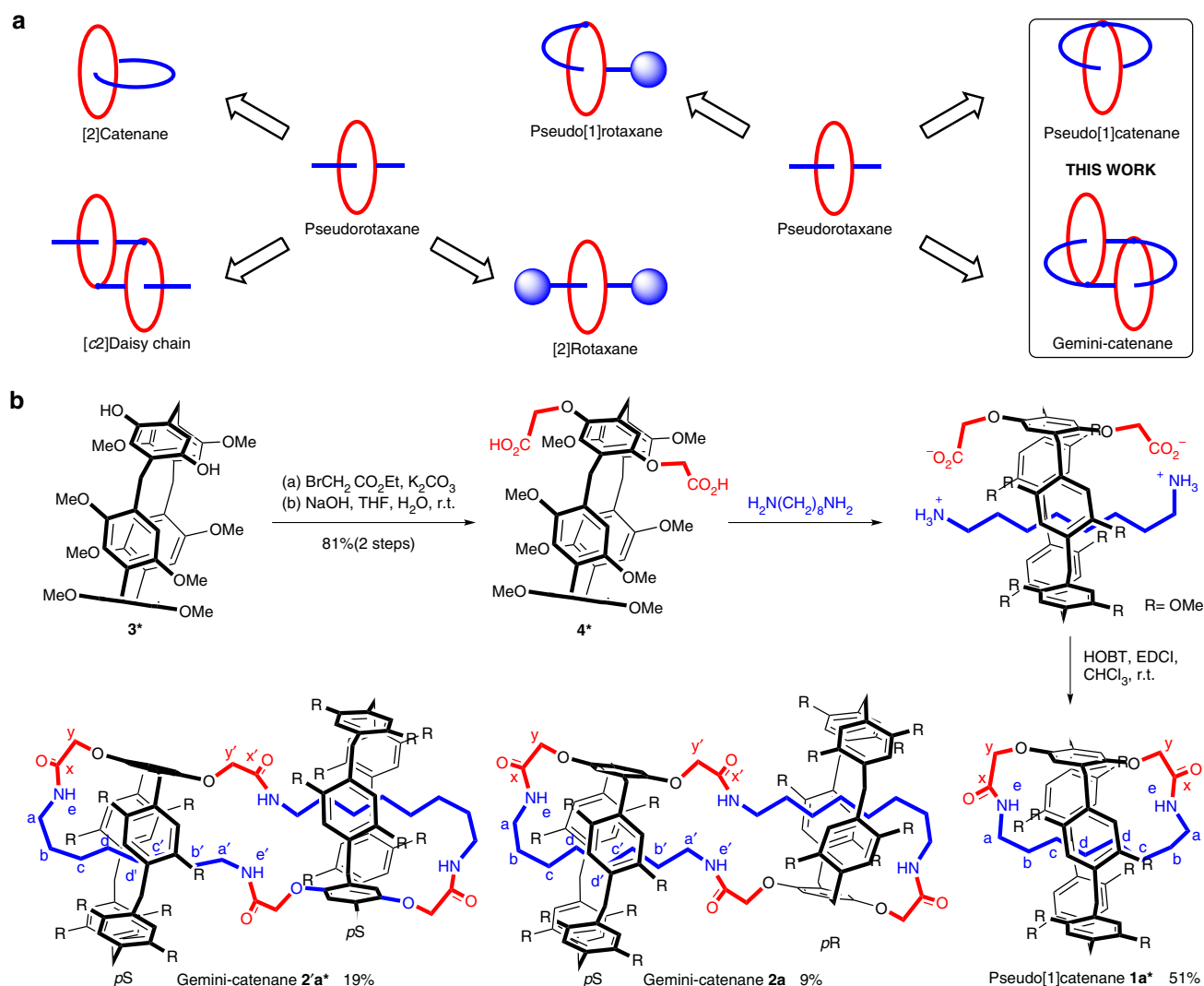


Figure 1 | Syntheses of pseudo[1]catenane and gemini-catenane. (a) MIMs and MSMs derived from pseudorotaxane. The original macrocyclic and acyclic components are indicated by red and blue colours, respectively. (b) Synthetic scheme of pseudo[1]catenane and gemini-catenane based on pillar[5]arene. *Only (*pS*)-enantiomers are shown for clarity purpose.

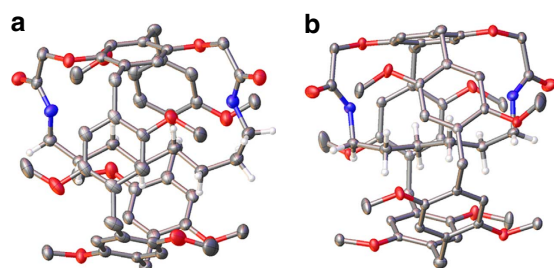


Figure 2 | Crystal structures of pseudo[1]catenanes. (a) Crystal structures of **1a**. (b) Crystal structures of **1d**. (Both of **1a** and **1d** the thermal ellipsoids are at 50% probability). In the crystal structure, the hydrogen atoms of the pillararene moiety were omitted for clarity purpose; colour code: carbons in grey, hydrogens of the octamethylene moiety in white, oxygens in red and nitrogens in blue.

erythro and the latter chiral threo. Figure 4c illustrates the UV/Vis and CD spectra of the first and second fractions of **2'a**, the absolute configurations of which were assigned to *pS* and *pR*, respectively, according to the same theoretical calculation of CD spectra of P[5]A⁴¹.

Although all the attempts to crystallize the gemini-catenanes were unsuccessful, as shown in Fig. 5, the DFT calculations revealed that **2a** is more stable than **2'a** by 0.8 kcal mol⁻¹. Interestingly, the Boltzmann distribution: **2'a**:**2a** = 3.7:1, evaluated by using the free energy difference, is close to relative isolated yield: 19%:9% = 2.1:1 (see Supplementary Methods and references for computational details).

Robust conformation of MSMs. In mechanically selflocked bicyclic structures, one of the incorporated macrocycles is often de-threaded from another macrocycle by aromatic ring tumbling^{23,24}. If such de-threading took place in our molecules, the proton signals of the octamethylene chain would coalesce in ¹H NMR spectra. In our case, no essential chemical shift changes were observed for any of the proton signals of pseudo[1]catenane **1a** in CDCl₃ even upon addition of an excess amount (10 equiv.) of competitor 1,4-dicyanobutane, which exhibits very strong binding affinities towards DMP[5]A⁴⁵, and the octamethylene proton signals were consistently upfield-shifted even in more polar CD₂Cl₂, CD₃CN and (CD₃)₂SO, as shown in Supplementary Fig. 30. We further performed the variable-temperature ¹H NMR experiment in (CD₃)₂SO to find no coalescence behaviour at least

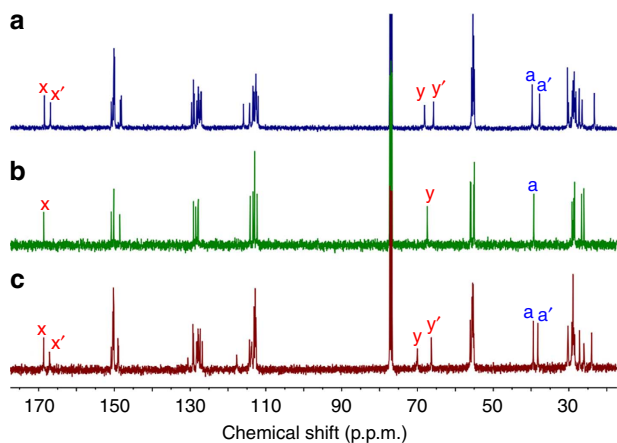


Figure 3 | Comparison of ^{13}C NMR spectra of MSMs. (a) ^{13}C NMR spectrum of **2'a** (100 MHz, CDCl_3 , 25 °C). (b) ^{13}C NMR spectrum of **1a** (100 MHz, CDCl_3 , 25 °C). (c) ^{13}C NMR spectrum of **2a** (100 MHz, CDCl_3 , 25 °C). The carbonyl (x) and adjacent methylene (a and y) carbons of pseudo[1]catenane **1a** are magnetically equivalent and show single peaks, while those of gemini-catenanes **2a** and **2'a** split into two peaks, reflecting the inequivalent magnetic environment.

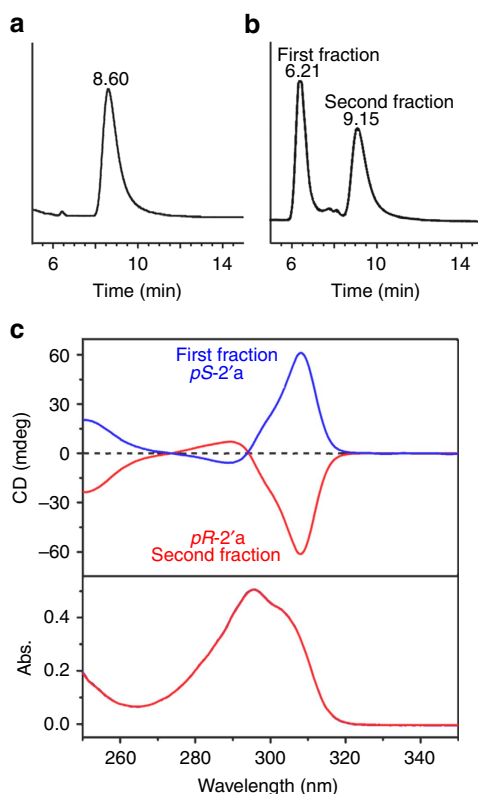


Figure 4 | Characterization of the chirality of gemini-catenane. (a) HPLC traces of **2a** on a chiral column. (b) HPLC traces of **2'a** on a chiral column. (c) UV/Vis and CD spectra of the first and second fractions. The existence of a single isomer in **2a** and a pair of enantiomers in **2'a** was confirmed by the chiral HPLC analyses and the mirror-imaged CD signals for the enantiomers of the latter ($[\rho\text{S-2'a}] = [\rho\text{R-2'a}] = 10 \mu\text{M}$ in CHCl_3 at 25 °C).

up to 80 °C. In addition, no new peaks (or products) were observed in the NMR spectrum of **1a** even after heating at 160 °C for 2 h. Exactly the same experiments were repeated with gemini-catenanes **2a** and **2'a** to show no essential changes in the NMR spectra (see

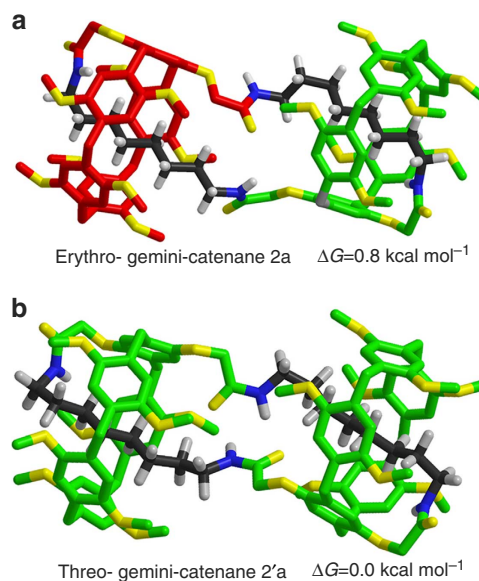


Figure 5 | Geometries and Gibbs free energies of gemini-catenanes **2a and **2'a** optimized by DFT calculations.** The geometries were optimized by using the B3LYP/6-31G(d) method. M062X-D3 dispersion energy corrections are included in the reported Gibbs free energies. The Gibbs free energy of **2a** is given relative to **2'a**. Hydrogen atoms of pillararene components are omitted for clarity. The (*pS*)- and (*pR*)-pillar[5]arenes are shown in green and red, respectively.

Supplementary Figs 32–37), indicating that the de-threading does not occur and hence **1a**, **2a** and **2'a** are conformationally robust. Nevertheless, there still remains the possibility of de-threading by tumbling one of the aromatic rings under extreme conditions, and hence we may describe them as pseudo[1]catenanes or endo-spirocycles.

Substrates scope with diaminoalkanes. The scope and limitations of this facile route to MSMs were explored by employing **DA-*n*** of shorter and longer methylene chain lengths ($n = 2-4, 6, 10$ and 12). As shown in Table 1, no catenanes were obtained in the reaction of **DA-2** with **4** (entry g), most probably due to the dimethylene linker, which is too short to catenate at the both ends of **4**. Possessing a longer methylene chain, **DA-3**, **DA-4** and **DA-6** (entries b–d) gave the corresponding pseudo[1]catenanes **1b**, **1c** and **1d** in progressively increasing 60, 86 and 96% yield, but no gemini-catenanes were obtained. The almost quantitative yield of **1d** may be attributed to the formation of highly stable pseudorotaxane **DA-6** \subset **4** (with a 10^5 M^{-1} order affinity⁴⁶), which is driven by the appropriate linker length for catenating cyclization and the dual electrostatic interactions⁴⁷ of the dicationic axle (diammoniohexane [**DA-6**· H_2]²⁺) with the dianionic wheel (pillararene-dicarboxylate 4^{2-}). However, such an ammonium-carboxylate pair is not favourable for amidation, because mechanistically the amidation pair should be charge-neutral. It is likely therefore that HOBT not only mediates the intermolecular amidation, but also stabilizes the guest in the pillararene cavity by forming a hydrogen-bond between the HOBT's nitrogen and the amino hydrogen on **DA-6**, as illustrated in Fig. 6. This leads to the smooth catenating amidation in the pseudorotaxane in particular for **DA-6**.

The use of longer diamine **DA-*n*** of $n \geq 8$ led to the sudden formation of gemini-catenanes **2** and **2'** at the expense of pseudo[1]catenane **1** (Table 1, entries a, e, f). With increasing methylene chain length (n), the yield of **1** markedly decreased from

performed on silica gel GF254 plates. Column chromatography was performed on silica gel (300–400 mesh). Melting points were measured on an RY-1A apparatus; the thermometer was not calibrated. ^1H NMR and ^{13}C NMR spectra were recorded on a Bruker AVANCE AV400 (400 and 100 MHz). Signal positions were reported in part per million (p.p.m.) relative to the residual solvent peaks or to the peak of $\text{Si}(\text{CH}_3)_4$ used as an internal standard with the abbreviations s, d, m, bs, and ABq, denoting singlet, doublet, multiplet, broad singlet and AB quartet, respectively. The residual ^1H peak of deuterated solvent appeared at 7.26 p.p.m. in CDCl_3 , at 5.32 p.p.m. in CD_2Cl_2 , at 1.94 p.p.m. in CD_3CN , and at 2.50 p.p.m. in $(\text{CD}_3)_2\text{SO}$, while the ^{13}C peak of CDCl_3 at 77.0 p.p.m. All coupling constants J are quoted in Hz. FTIR spectra were obtained with a Bruker Tensor 27 instrument. All IR samples were prepared as thin film and reported in wavenumbers (cm^{-1}). High resolution mass spectra (HRMS) were obtained on an Agilent 6520 Q-TOF LC/MS with ESI ionization. The X-ray diffraction data were collected by using a Rigaku Mercury CCD AFC10 system with monochromated Mo $K\alpha$ radiation. Chiral HPLC analyses were performed on an Agilent 6890 Series instrument. The dimensions of the HPLC columns are 4.6 mm diameter, and 250 mm length. Circular dichroism (CD) spectra were recorded on a BioLogic MOS500 spectropolarimeter in a quartz cell of 10 mm light path.

For ^1H and ^{13}C NMR spectra of compounds, see Supplementary Figs 1–28. For the comparisons of ^1H NMR spectra of the **1a**, **2a** and **2'a**, see Supplementary Fig. 29. For the variable deuterated solvents and temperatures of ^1H NMR spectra of **1a**, **2a** and **2'a**, see Supplementary Figs 30–37. For HRMS spectra of compounds, see Supplementary Figs 38–51. For IR spectra of compounds, see Supplementary Figs 52–65. For the chiral HPLC traces and CD spectra of **1a** and **2'a**, see Supplementary Figs 68–74. For crystallographic data of **1a** and **1d**, see Supplementary Table 1. Synthetic procedures and spectroscopic and physical data of compounds see Supplementary Methods. For the DFT calculations of gemini-catenanes of **2a** and **2'a**, also see Supplementary Methods. For the Cartesian coordinates (Å), SCF energies and Gibbs free energies at 298 K for the optimized structures of **2a** and **2'a**, see Supplementary Data 1.

Syntheses of MSMs. General procedures for the syntheses of pseudo[1]catenanes and gemini-catenanes: exemplified by the reaction of pillararene-dicarboxylic acid **4** with 1,8-diaminooctane **DA-8**: HOBT (101 mg, 0.75 mmol) and EDCI (144 mg, 0.75 mmol) were added to a solution of **4** (251 mg, 0.30 mmol) and **DA-8** (47 mg, 0.33 mmol) in chloroform (100 mL), and then the mixture was stirred for 48 h at room temperature. The reaction mixture was poured into 0.1 M aqueous HCl solution. The organic layer was washed with water, saturated aqueous NaHCO_3 solution and brine, dried over Na_2SO_4 and concentrated. The residue was purified by column chromatography on silica gel eluted with $\text{CHCl}_3/\text{MeOH}$ of 200:1 to 50:1 ratio (v/v) to afford **1a** as a white solid (120 mg, 51%); m.p. 290–292 °C; TLC ($\text{CHCl}_3/\text{MeOH}$ = 30:1 v/v), R_f = 0.65; ^1H NMR (400 MHz, CDCl_3) δ 6.97 (s, 2H), 6.87 (s, 2H), 6.84 (s, 4H), 6.80 (s, 2H), 5.85 (bs, 2H), 4.68, 4.48 (ABq, 4H), J = 16.4 Hz), 3.74–3.77 (m, 34H), 3.02 (bs, 2H), 2.80 (bs, 2H), 0.58–0.72 (m, 2H), 0.29–0.44 (m, 2H), –0.79 to –0.76 (m, 4H), –1.34 to –1.25 (m, 2H), –1.48 to –1.37 (m, 2H); ^{13}C NMR (100 MHz, CDCl_3) δ 168.7, 150.8, 150.2, 150.1, 148.6, 129.1, 128.5, 128.0, 127.9, 127.8, 114.2, 113.4, 113.0, 112.3, 67.4, 56.1, 55.9, 55.2, 55.0, 39.3, 29.2, 28.9, 28.7, 28.5, 26.7, 26.1; IR (KBr) ν_{max} 3,415, 2,934, 2,853, 2,829, 1,681, 1,496, 1,464, 1,398, 1,212, 1,046, 928, 880, 856, 774, 727, 704, 646 cm^{-1} ; HRMS (m/z): $[\text{M} + \text{H}]^+$ calc. for $\text{C}_{55}\text{H}_{67}\text{N}_2\text{O}_{12}$, 947.4694; found, 947.4670.

2a, White solid (21 mg, 9%); m.p. 294–296 °C; TLC ($\text{CHCl}_3/\text{MeOH}$ = 30:1 v/v): R_f = 0.57; ^1H NMR (400 MHz, CDCl_3) δ 6.86–6.97 (m, 20H), 6.73 (s, 2H), 5.08 (bs, 2H), 4.62, 4.55 (ABq, 4H), J = 16.4 Hz), 4.47, 4.39 (ABq, 4H), J = 16.4 Hz), 3.77–3.98 (m, 68H), 3.33 (bs, 2H), 3.23 (bs, 2H), 2.41 (bs, 2H), 1.69 (bs, 2H), 1.27 (bs, 4H), 0.62 (bs, 4H), –0.04 (bs, 4H), –1.01 (bs, 6H), –1.28 (bs, 2H), –1.97 (bs, 4H); ^{13}C NMR (100 MHz, CDCl_3) δ 168.7, 167.1, 150.9, 150.4, 150.2, 150.1, 149.1, 148.9, 130.6, 129.3, 129.1, 128.3, 128.2, 127.9, 127.7, 127.3, 126.8, 117.7, 114.4, 113.9, 113.7, 113.2, 112.9, 112.7, 112.6, 70.0, 66.3, 56.1, 55.6, 55.5, 55.4, 55.3, 55.2, 55.1, 39.4, 38.2, 30.4, 30.3, 30.2, 29.3, 29.0, 28.8, 28.7, 28.5, 27.2, 26.0, 24.0; IR (KBr) ν_{max} 3,412, 2,933, 2,853, 2,829, 1,727, 1,680, 1,533, 1,498, 1,465, 1,399, 1,212, 1,047, 929, 880, 855, 774, 727, 704, 647 cm^{-1} ; HRMS (m/z): $[\text{M} + \text{H}]^+$ calc. for $\text{C}_{110}\text{H}_{133}\text{N}_4\text{O}_{24}$, 1,894.9343; found, 1,894.9295.

2'a, White solid (44 mg, 19%); m.p. 260–262 °C; TLC ($\text{CHCl}_3/\text{MeOH}$ = 30:1 v/v): R_f = 0.52; ^1H NMR (400 MHz, CDCl_3) δ 6.84–7.05 (m, 20H), 6.84 (s, 2H), 5.23 (bs, 2H), 4.62 (s, 4H), 4.51 (s, 4H), 3.74–3.82 (m, 68H), 3.36 (bs, 4H), 2.67 (bs, 2H), 1.71 (bs, 2H), 1.47 (bs, 4H), 0.78 (bs, 4H), –0.08 (bs, 2H), –0.15 (bs, 2H), –1.09 (bs, 2H), –1.21 (bs, 2H), –1.45 (bs, 2H), –1.55 (bs, 2H), –2.33 (bs, 4H); ^{13}C NMR (100 MHz, CDCl_3) δ 168.5, 166.9, 150.8, 150.4, 150.2, 150.1, 150.1, 145.0, 148.4, 148.1, 129.6, 129.1, 128.9, 128.3, 127.9, 127.9, 127.7, 127.4, 127.2, 127.0, 115.9, 114.3, 113.4, 113.2, 112.8, 112.6, 112.5, 112.1, 68.1, 66.8, 55.7, 55.6, 55.4, 55.2, 55.1, 55.0, 39.7, 37.7, 30.4, 30.1, 29.1, 29.0, 28.7, 28.5, 28.2, 27.3, 26.6, 23.3; IR (KBr) ν_{max} 3,411, 2,935, 2,854, 2,829, 1,680, 1,532, 1,498, 1,465, 1,398, 1,212, 1,046, 928, 880, 855, 774, 731, 704, 647 cm^{-1} ; HRMS (m/z): $[\text{M} + \text{H}]^+$ calc. for $\text{C}_{110}\text{H}_{133}\text{N}_4\text{O}_{24}$, 1,894.9343; found, 1,894.9445.

References

- Frisch, H. L. & Wasserman, E. Chemical topology. *J. Am. Chem. Soc.* **83**, 3789–3795 (1961).
- Amabilino, D. B. & Perez-Garcia, L. Topology in molecules inspired, seen and represented. *Chem. Soc. Rev.* **38**, 1562–1571 (2009).
- Forgan, R. S., Sauvage, J.-P. & Stoddart, J. F. Chemical topology: complex molecular knots, links and entanglements. *Chem. Rev.* **111**, 5434–5464 (2011).
- Balzani, V., Credi, A. & Venturi, M. *Molecular devices and machines—concepts and perspectives for the nanoworld* (Wiley-VCH, 2008).
- Coskun, A., Banaszak, M., Astumian, R. D., Stoddart, J. F. & Grzybowski, B. A. Great expectations: can artificial molecular machines deliver on their promise? *Chem. Soc. Rev.* **41**, 19–30 (2012).
- Stijn, F. M. *et al.* Functional interlocked systems. *Chem. Soc. Rev.* **43**, 99–122 (2014).
- Lewandowski, B. *et al.* Sequence-specific peptide synthesis by an artificial small-molecule machine. *Science* **339**, 189–193 (2013).
- Beves, J. E., Blight, B. A., Campbell, C. J., Leigh, D. A. & McBurney, R. T. Strategies and tactics for the metal-directed synthesis of rotaxanes, knots, catenanes and higher order links. *Angew. Chem. Int. Ed.* **50**, 9260–9327 (2011).
- Barin, G., Forgan, R. S. & Stoddart, J. F. Mechanostereochemistry and the mechanical bond. *Proc. R. Soc. A* **468**, 2849–2880 (2012).
- Hänni, K. D. & Leigh, D. A. The application of CuAAC ‘click’ chemistry to catenane and rotaxane synthesis. *Chem. Soc. Rev.* **39**, 1240–1251 (2010).
- Pasini, D. The click reaction as an efficient tool for the construction of macrocyclic structures. *Molecules* **18**, 9512–9530 (2013).
- Liu, Y., Ke, C. -F., Zhang, H. -Y., Cui, J. & Ding, F. Complexation-induced transition of nanorod to network aggregates: alternate porphyrin and cyclodextrin arrays. *J. Am. Chem. Soc.* **130**, 600–605 (2008).
- Zhang, Z. -J., Zhang, H. -Y., Wang, H. & Liu, Y. A twin-axial hetero[7]rotaxane. *Angew. Chem. Int. Ed.* **50**, 10834–10838 (2011).
- Zhang, Z. -J., Han, M., Zhang, H. -Y. & Liu, Y. A double-leg donor–acceptor molecular elevator: new insight into controlling the distance of two platforms. *Org. Lett.* **15**, 1698–1701 (2013).
- Ashton, P. R. *et al.* Supramolecular daisy chains. *Angew. Chem. Int. Ed.* **37**, 1913–1916 (1998).
- Rotzler, J. & Mayor, M. Molecular daisy chains. *Chem. Soc. Rev.* **42**, 44–62 (2013).
- Bruns, C. J. *et al.* An electrochemically and thermally switchable donor–acceptor [c2]daisy chain rotaxane. *Angew. Chem. Int. Ed.* **53**, 1953–1958 (2014).
- Bruns, C. J. *et al.* Redox switchable daisy chain rotaxanes driven by radical–radical interactions. *J. Am. Chem. Soc.* **136**, 4714–4723 (2014).
- Hubin, T. J. & Busch, D. H. Template routes to interlocked molecular structures and orderly molecular entanglements. *Coord. Chem. Rev.* **200**, 5–52 (2000).
- Hiratani, K., Kaneyama, M., Nagawa, Y., Koyama, E. & Kanesato, M. Synthesis of [1]rotaxane via covalent bond formation and its unique fluorescent response by energy transfer in the presence of lithium ion. *J. Am. Chem. Soc.* **126**, 13568–13569 (2004).
- Li, H. *et al.* Dual-mode operation of a bistable [1]rotaxane with a fluorescence signal. *Org. Lett.* **15**, 3070–3073 (2013).
- Xia, B. & Xue, M. Design and efficient synthesis of a pillar[5]arene-based [1]rotaxane. *Chem. Commun.* **50**, 1021–1023 (2014).
- Wolf, R. *et al.* A molecular chameleon: chromophoric sensing by a self-complexing molecular assembly. *Angew. Chem. Int. Ed.* **37**, 975–979 (1998).
- Ogoshi, T., Akutsu, T., Yamafuji, D., Aoki, T. & Yamagishi, T. Solvent- and achiral-guest-triggered chiral inversion in a planar chiral pseudo[1]catenane. *Angew. Chem. Int. Ed.* **52**, 8111–8115 (2013).
- Liu, Y., Bonvallet, P. A., Vignon, S. A., Khan, S. I. & Stoddart, J. F. Donor–acceptor pretzelanes and a cyclic bis[2]catenane homologue. *Angew. Chem. Int. Ed.* **44**, 3050–3055 (2005).
- Han, M. *et al.* [2]Catenane and pretzelane based on Sn-porphyrin and crown ether. *Eur. J. Org. Chem.* **2011**, 7271–7277 (2011).
- Romuald, C., Arda, A., Clavel, C., Jimenez-Barbero, J. & Coutrot, F. Tightening or loosening a pH-sensitive double-lasso molecular machine readily synthesized from an ends-activated [c2]daisy chain. *Chem. Sci.* **3**, 1851–1857 (2012).
- Romuald, C., Cazals, G., Enjalbal, C. & Coutrot, F. Straightforward synthesis of a double-lasso macrocycle from a nonsymmetrical [c2]daisy chain. *Org. Lett.* **15**, 184–187 (2013).
- Boyle, M. M. *et al.* Stereochemistry of molecular figures-of-eight. *Chem. Eur. J.* **18**, 10312–10323 (2012).
- El-Faham, A. & Albericio, F. Peptide coupling reagents, more than a letter soup. *Chem. Rev.* **111**, 6557–6602 (2011).
- Hemantha, H. P., Narendra, N. & Sureshbabu, V. V. Total chemical synthesis of polypeptides and proteins: chemistry of ligation techniques and beyond. *Tetrahedron* **68**, 9491–9537 (2012).
- Stolze, S. C. & Kaiser, M. Challenges in the syntheses of peptidic natural products. *Synthesis* **44**, 1755–1777 (2012).
- Ogoshi, T., Kanai, S., Fujinami, S., Yamagishi, T. & Nakamoto, Y. para-Bridged symmetrical pillar[5]arenes: their Lewis acid catalyzed synthesis and host–guest property. *J. Am. Chem. Soc.* **130**, 5022–5023 (2008).

34. Cragg, P. J. & Sharma, K. Pillar[5]arenes: fascinating cyclophanes with a bright future. *Chem. Soc. Rev.* **41**, 597–697 (2012).
35. Xue, M., Yang, Y., Chi, X., Zhang, Z. & Huang, F. Pillararenes, a new class of macrocycles for supramolecular chemistry. *Acc. Chem. Res.* **45**, 1294–1308 (2012).
36. Ogoshi, T. & Yamagishi, T. Pillar[5]- and pillar[6]arene-based supramolecular assemblies built by using their cavity-size-dependent host-guest interactions. *Chem. Commun.* **50**, 4776–4787 (2014).
37. Strutt, N. L., Zhang, H., Schneebeli, S. T. & Stoddart, J. F. Functionalizing pillar[n]arenes. *Acc. Chem. Res.* **47**, 2631–2642 (2014).
38. Strutt, N. L. *et al.* Incorporation of an A1/A2-difunctionalized pillar[5]arene into a metal – organic framework. *J. Am. Chem. Soc.* **134**, 17436–17439 (2012).
39. Han, C., Zhang, Z., Yu, G. & Huang, F. Syntheses of a pillar[4]arene[1]quinone and a difunctionalized pillar[5]arene by partial oxidation. *Chem. Commun.* **48**, 9876–9878 (2012).
40. Ogoshi, T. *et al.* Clickable di- and tetrafunctionalized pillar[n]arenes (n = 5, 6) by oxidation – reduction of pillar[n]arene units. *J. Org. Chem.* **77**, 11146–11152 (2012).
41. Ogoshi, T. *et al.* High-yield diastereoselective synthesis of planar chiral [2]- and [3]rotaxanes constructed from per-ethylated pillar[5]arene and pyridinium derivatives. *Chem. Eur. J.* **18**, 7493–7500 (2012).
42. Schmieder, R., Hübner, G., Seel, C. & Vögtle, F. The first cyclodiastereomeric [3]rotaxane. *Angew. Chem. Int. Ed.* **38**, 3528–3530 (1999).
43. Cantrill, S. J., Youn, G. J., Stoddart, J. F. & Williams, D. J. Supramolecular daisy chains. *J. Org. Chem.* **66**, 6857–6872 (2001).
44. Coutrot, F., Romuald, C. & Busseron, E. A new pH-Switchable dimannosyl [c2]daisy chain molecular machine. *Org. Lett.* **10**, 3741–3744 (2008).
45. Shu, X. *et al.* Highly effective binding of neutral dinitriles by simple pillar[5]arenes. *Chem. Commun.* **48**, 2967–2969 (2012).
46. Yu, G., Hua, B. & Han, C. Proton transfer in host – guest complexation between a difunctional pillar[5]arene and alkyldiamines. *Org. Lett.* **16**, 2486–2489 (2014).
47. Capici, C. *et al.* Selective amine recognition driven by host – guest proton transfer and salt bridge formation. *J. Org. Chem.* **77**, 9668–9675 (2012).

Acknowledgements

Financial support was provided by the 973 Programme (2011CB932500) and the National Natural Science Foundation of China (Nos. 21432004, 21372128 and 91227107).

Author contributions

S.-H.L. and H.-Y.Z. performed the experiments and analysed the topological structures of pseudo[1]catenanes and gemini-catenanes. X.X. calculated the geometries and the Gibbs free energies of the gemini-catenanes. Y.L. supervised the work and edited the manuscript.

Additional information

Accession codes: For OLEX of products **1a** and **1d**, see Supplementary Figs 66 and 67. CCDC 1016257 and CCDC 1016258 contain supplementary crystallographic data for this paper. These data can be obtained free of charge from The Cambridge Crystallographic Data Centre via www.ccdc.cam.ac.uk/data_request/cif.

Supplementary Information accompanies this paper at <http://www.nature.com/naturecommunications>

Competing financial interests: The authors declare no competing financial interests.

Reprints and permission information is available online at <http://npg.nature.com/reprintsandpermissions/>

How to cite this article: Li, S.-H. *et al.* Mechanically self-flocked chiral gemini-catenanes. *Nat. Commun.* **6**:7590 doi: 10.1038/ncomms8590 (2015).



This work is licensed under a Creative Commons Attribution-NonCommercial-ShareAlike 4.0 International License. The images or other third party material in this article are included in the article's Creative Commons license, unless indicated otherwise in the credit line; if the material is not included under the Creative Commons license, users will need to obtain permission from the license holder to reproduce the material. To view a copy of this license, visit <http://creativecommons.org/licenses/by-nc-sa/4.0/>